JACC: CARDIOVASCULAR IMAGING VOL. 2, NO. 2, 2009

ISSN 1936-878X/09/$36.00
PUBLISHED BY ELSEVIER INC. DOI:10.1016/j.jcmg.2008.10.011

# Systematic Analysis of Functional and Structural Changes After Coronary Microembolization: A Cardiac Magnetic Resonance Imaging Study

Frank Breuckmann, MD,* Kai Nassenstein, MD,† Christina Bucher,* Ina Konietzka,‡ Gernot Kaiser, MD,§ Thomas Konorza, MD,* Christoph Naber, MD,* Andreas Skyschally, PhD,‡ Petra Gres,‡ Gerd Heusch, MD, FRCP,‡ Raimund Erbel, MD, FACC,* Jörg Barkhausen, MD†

*Essen, Germany*

**OBJECTIVES** Our study aimed to detect the morphological und functional effects of coronary microembolization (ME) in vivo by cardiac magnetic resonance (CMR) imaging in an established experimental animal model.

**BACKGROUND** Post-mortem morphological alterations of coronary ME include perifocal inflammatory edema and focal microinfarcts. Clinically, the detection of ME after successful coronary interventions identifies a population with a worse long-term prognosis.

**METHODS** In 18 minipigs, ME was performed by intracoronary infusion of microspheres followed by repetitive in vivo imaging on a 1.5-T MR system from 30 min to 8 h after ME. Additionally, corresponding ex vivo CMR imaging and histomorphology were performed.

**RESULTS** Cine CMR imaging demonstrated a time-dependent increase of wall motion abnormalities from 9 of 18 animals after 30 min to all animals after 8 h (0.5 h, 50%; 2 h, 78%; 4 h, 75%; 8 h, 100%). Whereas T2 images were negative 30 min after ME, 4 of 18 animals showed myocardial edema at follow-up (0.5 h, 0%; 2 h, 6%; 4 h, 25%; 8 h, 17%). In vivo late gadolinium enhancement (LGE) was observed in none of the animals after 30 min, but in 33%, 50%, and 83% of animals at 2 h, 4 h, and 8 h, respectively, after ME. Ex vivo CMR imaging showed patchy areas of LGE in all but 1 animal (2 h, 83%; 4 h, 100%; 8 h, 100%). A significant correlation was seen between the maximum troponin I level and LGE in vivo ($r = 0.63$) and the spatial extent of ex vivo LGE ($r = 0.76$).

**CONCLUSIONS** Our results show that in vivo contrast-enhanced CMR imaging allows us to detect functional and structural myocardial changes after ME with a high sensitivity. Ex vivo, the pattern of LGE of high-resolution, contrast-enhanced CMR imaging is different from the well-known pattern of LGE in compact myocardial damage. Thus, improvements in spatial resolution are thought to be necessary to improve its ability to visualize ME-induced structural alterations even in vivo. (J Am Coll Cardiol Img 2009;2:121–30) © 2009 by the American College of Cardiology Foundation

From the Departments of *Cardiology and †Diagnostic and Interventional Radiology and Neuroradiology, and the ‡Institute of Pathophysiology, West German Heart Center, Essen, Germany; and the §Department of General, Visceral and Transplantation Surgery, University Duisburg-Essen, Essen, Germany. This study was supported by the German Research Foundation (Deutsche Forschungsgemeinschaft, grant BA 2115/2-1). Dr. Heusch was supported for his studies on coronary microembolization by the German Research Foundation (Deutsche Forschungsgemeinschaft, grant HE 1320/14-1).

Manuscript received May 28, 2008; revised manuscript received October 21, 2008, accepted October 27, 2008.

Coronary microembolization (ME) has been identified as a potential source of myocardial dysfunction, malignant arrhythmias, and reduced coronary flow reserve, which may result in fatal consequences (1,2). Therefore, several experimental and clinical studies have investigated the morphological and functional effects of ME. In controlled animal experiments, the immediate consequences of ME include a transient decrease of coronary blood flow, subsequent reactive hyperemia, and a moderate reduction in myocardial wall function, followed by progressive and more severe myocardial dysfunction or recovery over time (3–7). Histological examinations after ME show inflammatory reactions, perifocal myocardial edema, and focal microinfarcts.

Interestingly, ME has been frequently documented at autopsy in patients with stable and unstable angina who suffered sudden cardiac death (8–11). Additionally to spontaneous ME, it may also occur in the course of coronary interventions. Periinterventional ME seems to be reflected indirectly by an increase in cardiac biomarkers including troponin I and creatine kinase-myocardial band, electrocardiographic alterations, or impairment of microvascular perfusion up to a full no-reflow phenomenon (12–14). Clinically, the detection of ME after successful coronary interventions identifies patients with a worse long-term prognosis compared with patients with no enzyme elevations (15). In vivo evidence for ME may be obtained from debris and soluble substances retrieved from filtration and aspiration protection as well as from Doppler ultrasonography evaluation (14,16–19), but direct visualization of the myocardial damage in vivo is challenging.

**ABBREVIATIONS AND ACRONYMS**

**BW** = body weight
**CMR** = cardiac magnetic resonance
**ED** = end-diastole
**ES** = end-systole
**IR-FLASH** = inversion recovery turbo fast low-angle shot
**LGE** = late gadolinium enhancement
**ME** = coronary microembolization
**RF** = radiofrequency
**SSFP** = steady-state free precession
**TSE** = T2-weighted turbo spin echo

In principle, cardiac magnetic resonance (CMR) imaging should be able to visualize the effects of coronary ME in vivo because steady-state free precession (SSFP) cine sequences allow for the assessment of wall motion abnormalities whereas T2-weighted turbo spin echo (TSE) sequences and the late gadolinium enhancement (LGE) technique provide morphological information about myocardial damage. Inflammatory reactions as well as focal infarcts caused by ME should result in increased signal intensity on T2-weighted images and should lead to contrast enhancement due to an increased distribution volume for low-molecular agents in the steady state after contrast injection (20).

Recently, contrast-enhanced CMR imaging has been used to detect periprocedural myocardial necrosis in patients (21,22). Focal areas of late gadolinium enhancement were detected after percutaneous coronary intervention, and the extent of LGE showed a good correlation with troponin I and creatine kinase-myocardial band elevations. Distal ME and stent-related side-branch occlusion with different patterns of LGE have been proposed as possible sources of biomarker elevation (23,24). Additionally, Selvanayagam et al. (25) have recently shown that the reduced myocardial perfusion reserve index can be assessed in vivo quantitatively by first-pass perfusion CMR imaging.

However, in clinical studies, the early effects of ME cannot be studied over time, and a histological verification cannot be performed. Additionally, stent-related side-branch occlusions may result in small infarcts rather than ME, overlapping with the effects of coronary ME. Therefore, our study aimed to evaluate the effects of ME over time using contrast-enhanced CMR imaging in an established experimental animal model.

## METHODS

**Setting.** Experiments were performed in 18 male Göttinger minipigs (Ellegaard, Dalmose, Denmark), weighing 23 to 41 kg, according to the "Guidelines for Humane Care and Use of Animals," as published by the National Institutes of Health (NIH publication 85-23, revised 1996), and approved by the Bioethical Committee of the District of Duesseldorf, Germany. After sedation using intramuscular injection of ketamine (30 mg/kg body weight [BW]), azaperone (2 mg/kg BW), and atropine (0.025 mg/kg BW), initiation of anesthesia by intravenous fentanyl (0.005 mg/kg BW), thiopental (12.5 mg/kg BW), and midazolam (0.15 mg/kg BW) was followed by endotracheal intubation. Anesthesia was maintained by continuous thiopental infusion (10 mg/kg BW) as well as by additional bolus administration of fentanyl (0.0025 mg/kg BW) and midazolam (0.25 mg/kg BW) according to the reflex status of the pig (26). Continuous monitoring included heart rate and electrocardiogram via external leads, oxygenation via peripheral oxygen sensors, and invasive blood pressure measurements. Arterial blood gases were analyzed frequently after intubation and during ME and then periodically throughout the study.

**CMR imaging.** All examinations were performed on a 1.5-T scanner (Espree Magnetom, Siemens Med-

ical Solutions, Erlangen, Germany) using electrocardiographic triggering and breath-hold sequences. Animals were placed head first in supine position on top of the spine-array radiofrequency (RF) coil build into the table. Additionally, a body phased-array RF receiver coil was placed on top of the animal's chest. SSFP cine CMR imaging for wall motion analysis (TR 3 ms, TE 1.5 ms, FA 60°, resolution 1.3 × 1.3 × 6 $mm^3$), fat-suppressed triple inversion recovery T2-weighted dark-blood–prepared TSE CMR imaging to visualize myocardial edema (TR 2 heart beats, TE 59 ms, FA 180°, resolution 1.3 × 1.7 × 5 $mm^3$, bandwidth 235 Hz/pixel) as well as inversion recovery turbo fast low-angle shot (IR-FLASH) for the assessment of LGE (TR 8 ms, TE 4 ms, TI 240-320 ms, FA 20°, resolution 1.3 × 1.7 × 5 $mm^3$) 10 min after administration of 0.2 mmol/kg Gd-DTPA (Magnevist, Schering, Berlin) were performed before coronary catheterization as internal control.

**Microembolization.** A longitudinal incision on the left side of the neck for preparation of the carotid artery for coronary catheterization and the jugular vein for volume replacement and medications was performed. Catheter sheaths (6-F) were implanted and fixed. All pigs were fully heparinized after the implantation of the sheaths for the duration of the experiments.

After intubation of the left coronary artery with a XB-3 coronary catheter (Cordis Neurovascular, Miami, Florida), insertion of a coronary wire (Floppy Wire, Guidant, Santa Clara, California), and advancement of a 2.3-F infusion microcatheter (Prowler Plus, Cordis Neurovascular), ME was induced by injection of white-colored polystyrene microspheres (42-$\mu$m diameter, Dynospheres, Dyno Particles, Lillestrom, Norway) to the left coronary artery, as previously described (4). In 17 cases, the microcatheter was placed into the distal portion of the left anterior descending coronary artery under radiographic guidance. In 1 case, the distal left circumflex coronary artery was chosen because of a hypoplastic left anterior descending coronary artery. To avoid clumping, microspheres were infused in suspension of 1 × $10^6$/ml saline with 0.02% Tween 80 by slow 1.5 ml/min manual injection after adequate stirring, corresponding to approximately 4,500 microspheres per ml/min estimated coronary flow, as determined by previous studies in minipigs of the same weight (7). Infusion of microspheres was followed by a 5-ml heparinized saline flush.

**In vivo CMR imaging after ME.** After ME, the animals were immediately transferred to the CMR scanner and repositioned, as described before. In 6 animals, SSFP cine, T2-weighted TSE, and IR-FLASH sequences were performed 30 min as well as 2 h after ME, followed by euthanasia. In 6 animals, the MR protocol was performed 30 min and 2 and 4 h after ME, whereas in the last group (6 animals), the protocol lasted 8 h with an additional CMR examination 8 h after ME. At all imaging time points, 0.2 mmol/kg Gd-DTPA was injected 10 to 15 min before the acquisition of the IR-FLASH sequences.

**Troponin I.** Blood samples were obtained shortly before experimental ME and up to 8 h after ME, respectively. Troponin I serum levels (ng/ml) were determined by routine laboratory procedures (Dade Behring, Eschborn, Germany).

**Ex vivo preparation.** Animals were euthanized by intravenous bolus injection of 80 mg/kg BW pentobarbital. The heart was sectioned from base to apex into 4 to 5 slices in a plane parallel to the atrioventricular groove, and each slide was placed in the middle of a 2-element 4-channel carotid phased-array RF coil (Machnet, Eelde, the Netherlands) for signal reception. High-resolution ex vivo CMR imaging using IR-FLASH sequences (TR 8 ms, TE 4 ms, TI 240 to 320 ms, resolution 0.5 × 0.5 × 2 $mm^3$) of the explanted heart was achieved slice by slice from base to apex.

**Histology.** Each slice from the basis to the apex was fixed in formalin immediately after high-resolution ex vivo scanning. Representative tissue blocks (approximately 0.5 × 1 × 1 $cm^3$) of the target area, with LGE detected by ex vivo CMR imaging, as well as the control area (no LGE) were embedded in paraffin, cut in 5-$\mu$m specimens, mounted on slides, and stained with hematoxylin-eosin. Specimens were analyzed for the presence of microspheres and of perifocal inflammatory infiltrates. Microinfarcts were evaluated as the mean percentage of the total left ventricular area per field of view (magnification ×100, mean area 108 ± 34 $mm^2$) (27).

**Wall motion, wall thickening, edema, and GE CMR imaging analysis.** All CMR imaging examinations were evaluated by 2 radiologists and 1 cardiologist in consensus. Regional wall motion was evaluated visually and characterized as normal, hypokinetic, akinetic, or dyskinetic. For quantification of regional wall motion thickening within the target volume (anterior, anteroseptal, and septal wall) the thickness of the left ventricular myocardium was

measured at end-diastole (ED) and end-systole (ES) within the target segments 1, 2, 7, 8, 13, and 14 and within segments 5, 6, 11, 12, and 16 as internal controls, both according to the 17-segment model of the American Heart Association (28). Systolic wall thickening was calculated and normalized to the control zone to account for potential effects of anesthesia of >8 h on left ventricular function ([ES thickness − ED thickness of the target area] / [ES thickness − ED thickness of the control area]). The T2-weighted images were visually evaluated for the presence or absence of myocardial edema. In vivo and ex vivo LGE images were visually assessed (presence vs. absence of LGE). Based on ex vivo images, the expansion of LGE ($mm^2$) was calculated by in-house developed software. In brief, the mean signal intensity was measured within the remote area. Subsequently, target segments of the same slice were selected, and the total area exhibiting a signal intensity of more than the control mean plus 2 SD was determined automatically.

**Statistics.** All analyses were performed with the use of SPSS version 12.0 (SPSS Inc., Chicago, Illinois). Data are reported as mean ± SD (regional wall thickening index, signal intensity) or median and range (troponin I), respectively. The time course of regional wall thickening was analyzed by 1-way analysis of variance. Troponin I levels between in vivo LGE positive and negative animals were compared by the Wilcoxon rank sum test. Linear regression and Pearson correlation analyses were performed for troponin I levels versus wall thickening and for troponin I levels versus the extent of LGE ex vivo. A p value of <0.05 was taken to indicate significance. The authors had full access to and take full responsibility for the integrity of the data. All authors have read and agree to the manuscript as written.

## RESULTS

Experimental ME was successfully initiated in all animals. Anesthesia was well tolerated. Blood gases, heart rate, and blood pressure were kept within normal ranges throughout the duration of experiments and optimized by slight adjustment of ventilation parameters when necessary.

**Wall motion and wall thickening.** Using visual binary assessment, regional wall motion abnormalities of the target area were detected in 16 of the 18 animals (Group 1, n = 5 of 6; Group 2, n = 5 of 6; Group 3, n = 6 of 6) (Fig. 1A). In the first series of post-ME sequences, which were completed approximately 30 min after ME, regional wall thickening of the target area was reduced. Two 2 h after ME, wall thickening slightly improved, followed by a progressive decrease at 4 and 8 h after ME (Fig. 2).

**Myocardial edema.** The T2-weighted TSE sequences showed an increased signal intensity of the target segments in 4 of the 18 animals (Group 1; n = 1 of 6; Group 2, n = 2 of 6; Group 3, n = 1 of 6) (Fig. 1B). A weak, homogenous hyperintense signal with subendocardial to transmural extension was detected in all 4 cases.

**LGE in vivo.** In the latest LGE measurement in each group, in vivo IR-FLASH sequences revealed regional hyperenhancement of the target area in a total of 9 pigs (Group 1, n = 1/6; Group 2, n = 4/6; Group 3, n = 5/6) (Fig. 1C). There was an increase in the percentage of LGE positive animals over time, with a maximum of 83% after 8 h. Hyperintensity could be described as weak, characterized by enhancement with diffuse uptake mainly within the mid-myocardial layers (Fig. 3C).

**LGE ex vivo.** High-resolution ex vivo IR-FLASH revealed hyperenhancement within the target segments in all but 1 animal (Group 1, n = 5 of 6; Group 2, n = 6 of 6; Group 3, n = 6 of 6) (Fig. 1D). The signal distribution varied between focal patchy areas of LGE areas in only 1 segment (signal intensity 197.2 ± 50.2) (Fig. 3B) and more diffuse transmural areas of LGE in 1 or more segments (signal intensity 66.9 ± 18.6) (Fig. 3D).

**Histology.** There was no evidence for myocardial infarction or microinfarction in the remote area. In the microembolized areas of the LCA, microspheres were present throughout all sections. After 2 h, perifocal mononuclear infiltration and focal eosinophils were visible. Infarcted areas remained below 1% per section (mean 0.29 $mm^2$ microinfarcts per section) within the target area at this very early point of time. Histology of the pigs euthanized after 4 h revealed microinfarction with infiltrating leukocytes. Infarcted areas within the target segments remained between 1% and 3% per section (mean 2.01 $mm^2$ microinfarcts per section) (Fig. 4). After 8 h, when there was a clear demarcation of microinfarcts, the aggregate infarct size of the target area per section was 3% (mean 4.19 $mm^2$ microinfarcts per section).

**Troponin I.** Baseline troponin I was 0.02 (0 to 0.91) ng/ml. At 2 h after ME, troponin I increased to 0.33 (0.11 to 0.86) ng/ml (p = 0.01), at 4 h after

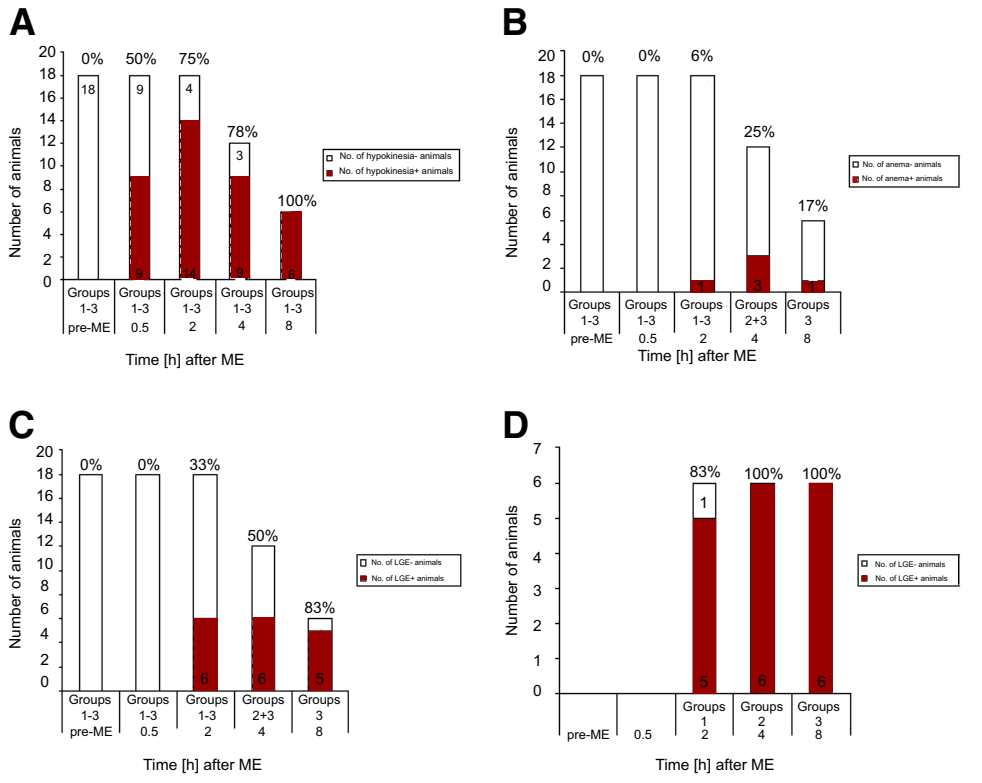


**Figure 1. Development of Visual Regional Contractile Dysfunction, Edema, In Vivo LGE, and High-Resolution Ex Vivo LGE After ME**

Development of visual regional contractile dysfunction **(A)**, edema **(B)**, in vivo late gadolinium enhancement (LGE) **(C)**, and high-resolution ex vivo LGE **(D)** in the time course after coronary microembolization (ME). Note: 1) that after 8 h, all animals exhibited regional hypokinesia; 2) the increase of in vivo LGE positive animals began 2 h after microsphere application; and 3) that even 2 h after ME, 5 of 6 animals were positive for ex vivo LGE, and 4 and 8 h after ME, LGE was observed in all animals. The T2 imaging was unable to serve as an independent method to detect very early stages of discrete intramyocardial edema.

ME, to 1.59 (0.32 to 4.21) ng/ml, and at 8 h after ME, to 2.30 (0.86 to 5.15) ng/ml ($p < 0.01$ both).

Increasing troponin I values tended to be associated with regional wall thickening impairment ($r = -0.39$, $p > 0.05$) (Fig. 5A). The median troponin I level in pigs with positive in vivo LGE was 2.7 (0.3 to 5.2) ng/ml, whereas in pigs without in vivo LGE, it was 0.4 (0.1 to 1.6) ng/ml ($p = 0.01$) (Fig. 6). Maximum troponin I after ME correlated with the area of ex vivo LGE ($r = 0.76$, $p < 0.01$) (Fig. 5B). There was no association between troponin I levels and the occurrence of myocardial edema ($p > 0.05$).

## DISCUSSION

ME has been investigated by CMR imaging in multiple clinical studies (21–25). However, in contrast to these clinical CMR imaging studies on peri-interventional myocardial damage, we used an established experimental model and were therefore able to exclude stent-related side-branch occlusion as a mechanism of injury. Additionally, we investigated early ME-induced myocardial damage over time noninvasively in vivo, including morphological and functional parameters, and the results of in vivo LGE imaging were verified by ex vivo high-resolution LGE imaging and histology. Our sequential CMR imaging analyses detecting immediate and subacute consequences of ME in an established experimental pig model underline the following: 1) In vivo LGE permits the visualization of ME-induced myocardial damage in up to 83% after 8 h. Ex vivo high-resolution LGE detects even small areas of microinfarction. The improvement in spatial resolution seems to be the key to improve the diagnostic accuracy of CMR imaging. 2) In vivo T2-weighted TSE sequences fail to visualize myocardial edema after ME in vivo. 3) SSFP cine CMR imaging can detect ME-induced contractile dysfunction noninvasively. The time window of con-

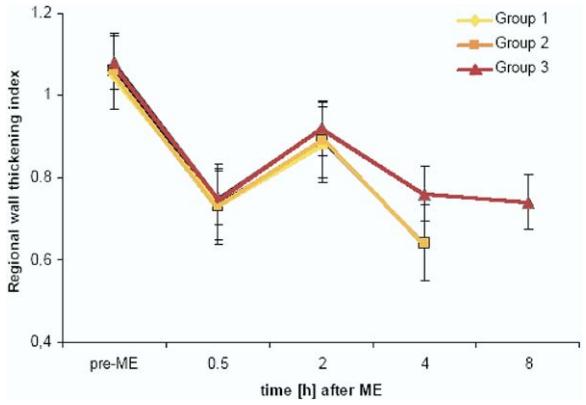


**Figure 2. Development of Regional Contractile Dysfunction After ME**

There is an early decrease of regional contractile function, followed by a slight recovery after 2 h and a further increase of wall motion dysfunction of the target segments during the subsequent 6 h. Regional wall thickening is expressed as the ratio of maximal thickening between the target area and the control area ([ES thickness − ED thickness of the target area] / [ES thickness − ED thickness of the control area]). Group 1 = **diamonds**; Group 2 = **squares**; Group 3 = **triangles**. ED = end-diastolic; ES = end-systolic; ME = coronary microembolization.

tractile dysfunction detected by CMR imaging resembles the results of echocardiographic patterns in animal studies using ultrasonic dimension gauges in open chest preparation.

LGE is based on an increased distribution volume for gadolinium chelates given intravenously ≈10 to 15 min before examination. The LGE occurs in regions of inflammation and edema, but also in areas of myocardial necrosis, both commonly regarded as key elements of ME (29).

In the present study, in vivo LGE was detected already 2 h after ME. The percentage of in vivo LGE positive animals increased during the following 6 h. LGE appeared with weak enhancement and diffuse signal intensity. To further characterize animals with positive in vivo LGE, troponin I levels of LGE-positive pigs were compared with those of LGE-negative animals (Fig. 6). The median troponin I value in pigs with positive LGE was higher than in those without LGE, suggesting a relation between LGE and total myocardial damage. Unlike in vivo CMR imaging, ex vivo imaging revealed

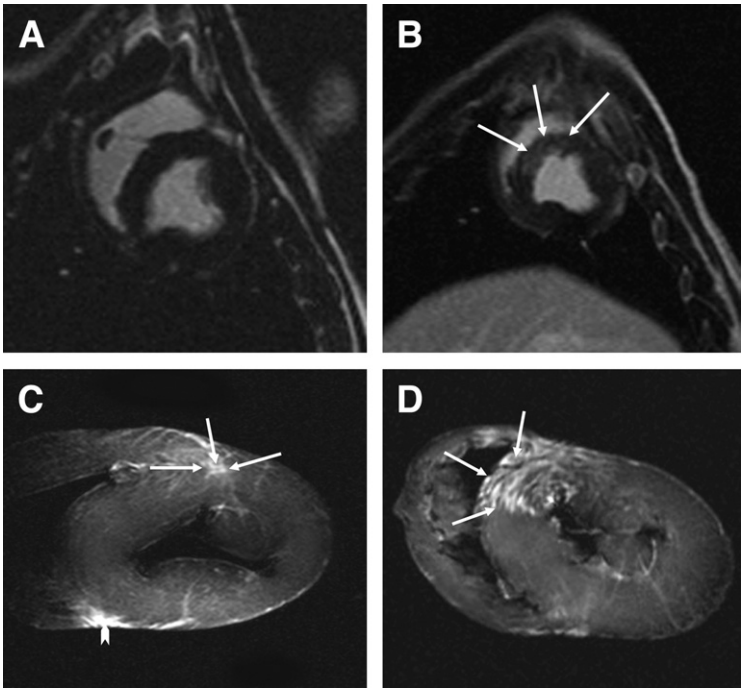


**Figure 3. Mid-Ventricular to Apical Short Axis In Vivo and Ex Vivo LGE Images**

Mid-ventricular to apical short axis in vivo late gadolinium enhancement (LGE) images **(A, B)** and ex vivo LGE images **(C, D)**. Whereas in a number of animals, in vivo LGE was negative **(A)**, in individual animals, even in vivo post-procedural focal spotted patchy to streaky subendocardial to mid-myocardial delayed enhancement was observed **(B, arrows)**. High-resolution ex vivo LGE showed different aspects of hyperenhancement. The signal varied between focal patchy areas of LGE in only 1 segment **(C, arrows)** and more diffuse transmural areas of LGE in 1 or more segments **(D, arrows)**, possibly due to a different distribution pattern of microspheres (**arrowhead** marks artifact of an epicardial vessel with remaining intravascular contrast agent post-mortem).

areas of LGE in all but 1 animal. In contrast to in vivo imaging, which revealed diffuse high signal intensity areas of LGE, ex vivo imaging showed streaky areas of LGE with high signal intensity within normal-appearing myocardium. Thus, ex vivo CMR imaging demonstrated that the diffuse LGE signal in the relatively low resolution in vivo images results from streaks of LGE with interposition of normal myocardium. Obviously, the differences between pattern and incidence of LGE in vivo and ex vivo after ME are predominantly caused by the substantially lower spatial resolution of in vivo imaging.

In previous studies, Ricciardi et al. (21) were the first to report the occurrence of focal LGE after angioplasty and stent implantation. Later, Selvanayagam et al. (23) were the first to propose a linear correlation between post-interventional troponin I elevation and the presence of LGE. Corresponding to the findings of the latter authors, we also found an association between troponin I elevations reflecting myocardial necrosis and the presence, and even the extent, of post-interventional LGE. However, our observed patterns of LGE in vivo and ex vivo are somewhat different to the findings of Ricciardi et al. (21). Apart from the occlusion of side branches, distal embolization of atheromatous plaque material during stent implantation was proposed as a mechanism underlying LGE (24). Contrary to our experimental observations, the authors described transmural to subendocardial areas of LGE with high signal intensities in the apical myocardium after assumed distal embolization. The most likely explanation for these differences seems to be that, in the clinical setting, the difference between side-branch occlusion and ME cannot be really ascertained. Thus, some areas of compact LGE may have been misinterpreted as resulting from distal ME. Another explanation is a potentially more compact distal embolization due to a higher plaque burden and a more heterogeneous particle size up to >100 $\mu$m in diameter in the study group of Ricciardi et al. (21). In support of this notion, Porto et al. (24) reported a significant correlation between changes in plaque volume and the mass of post-interventional focal myocardial necrosis. Thus, our data indicate that even ME by a limited number and small particle size of microemboli can be visualized by CMR imaging. Finally, the differences may also result from

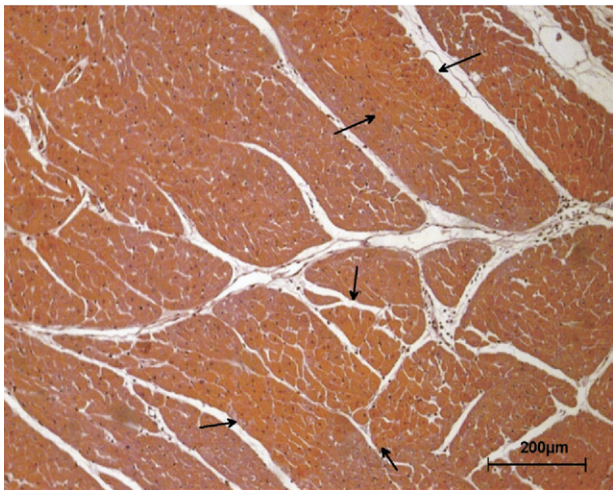


**Figure 4. Histology of Microinfarction**

Representative histomorphology even 4 h after microembolization showing focal small conglomerates of necrotic cardiomyocytes **(arrows)** and progressive inflammatory infiltration.

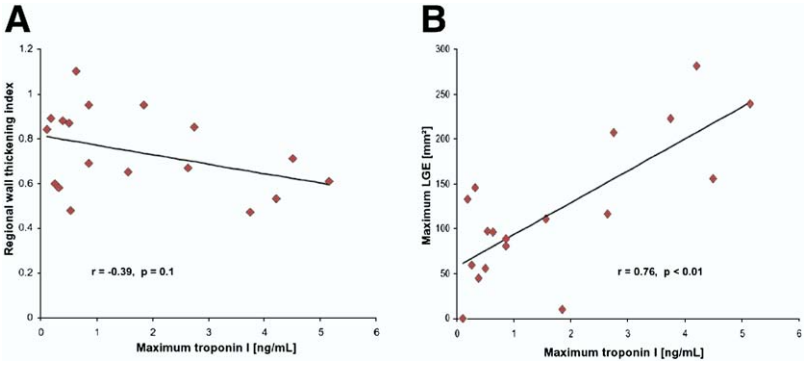


**Figure 5. Correlation of Wall Thickening and Ex Vivo LGE Versus Troponin I Levels**

Increasing troponin I levels tended to correlate with regional contractile dysfunction of the target segments **(A)** and correlated with maximum ex vivo late gadolinium enhancement (LGE) extension **(B)**.

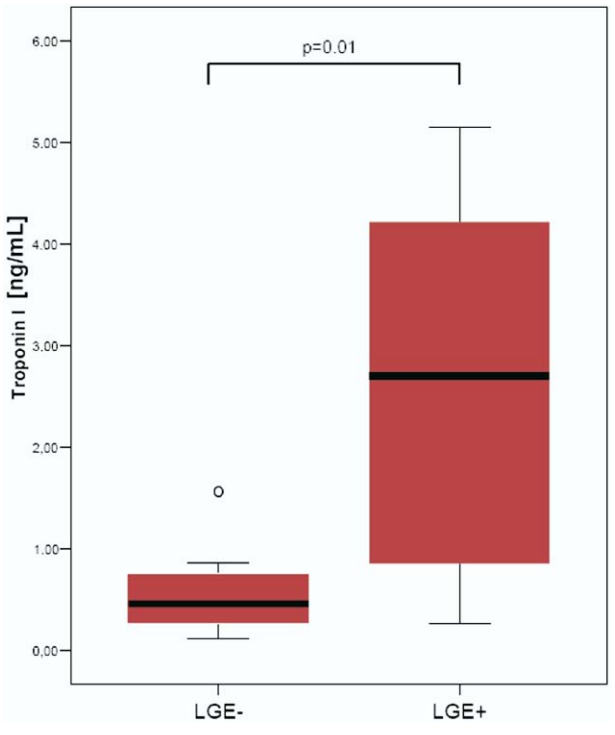


**Figure 6. Higher Troponin I in LGE-Positive Animals**

The box-plot diagram of maximum troponin I levels in late gadolinium enhancement (LGE)-positive and LGE-negative animals in vivo shows a greater increase of troponin I in pigs with LGE than in those without LGE.

the different time points for imaging, as the appearance of LGE areas may differ 24 h after ME compared to ≤8 h after ME.

Our experimental results also indicate that the distribution of ME influences the pattern of LGE: in animals with a small total area of LGE, the area of hyperenhancement was much brighter, compact, and focal. Thus, subendocardial LGE of high signal intensity such as reported by previous studies may be caused by multiple closely adjacent necrotic foci, and may, therefore, be only an exceptional case after ME. In the majority of cases, the signal of LGE was spotted to streaky, weak, and diffuse. Therefore, in clinical routine, these changes may be misconstrued to be artifacts. Thus, improved spatial resolution, for example, by imaging at high field strengths or by the use of navigator sequences, is necessary to reliably visualize structural changes after ME.

In contrast to regional contractile dysfunction, increased signal intensity on T2-weighted images, indicating myocardial edema, was detected only in a small number of animals. However, in all animals with an increased signal intensity on T2-weighted images, the hyperintense areas matched the areas of contractile dysfunction. It has been shown that myocardial edema can reliably be detected in acute myocardial infarction, and that T2-weighted sequences are helpful to distinguish acute and chronic myocardial damage (20). However, in our study T2-weighted sequences were unable to detect early stages of discrete focal intramyocardial edema within the first 8 h after ME in the majority of cases. It is well known that the contrast between damaged and normal myocardium is lower on T2-weighted images compared with contrast-enhanced scans. Thus, we believe that in most cases currently available sequences for myocardial edema imaging are not sensitive enough to detect such small areas of edema. Nevertheless, recently described T2-weighted steady-state free precession sequences may improve the image quality and robustness of T2-weighted sequences and may enhance the detection rate of focal myocardial edema in the near future (30). So far, it is well known that T2 TSE images are prone to artifacts; because the contrast between edema and normal myocardium is very low in cases with evidence for edema in T2-weighted images, semiquantitative assessment of myocardial edema was omitted.

Impairment of systolic wall thickening is a sensitive marker of myocardial ischemia, including ME. In our in vivo pig model, a regional reduction in wall motion was observed visually in all animals 8 h after ME, which was confirmed in the quantitative analysis as a significant decrease of wall thickening in the target segments. The observed time-dependent changes are in accordance with reported systolic wall thickening in microembolized pigs when using sonomicrometry (5–7). Thus, our data underline the potential of noninvasive functional CMR imaging in the detection of ME-induced wall motion impairment.

**Study limitations.** We used a rather simple model of ME in healthy nonatherosclerotic swine, and it remains unclear to what extent our experimental model reflects the clinical scenario with regard to size and number of microthromboembolic material and its relevant proinflammatory capability. However, in the clinical scenario, we suggest even higher myocardial damage as to the additional liberation of soluble substances and the heterogeneity of corpuscular fragment size (different from the homogenous 42-$\mu$m microspheres used in our study). Additionally, our experimental setting allows no estimation of the prognostic value of LGE after ME.

## CONCLUSIONS

Cine SSFP CMR imaging sequences can detect even early stages of contractile dysfunction with a high sensitivity. Therefore, the careful analysis of wall motion abnormalities seems to be 1 key for the detection of ME in vivo by CMR imaging. In vivo T2-weighted imaging failed in the detection of ME owing to its low sensitivity. High-resolution ex vivo imaging showed that contrast-enhanced CMR imaging is able to detect ME, and that the pattern of LGE after ME is different from the well-known pattern of LGE in compact myocardial damage (e.g., myocardial infarction). However, our results additionally show that the diagnostic accuracy of in vivo late enhancement imaging is limited predominantly because of its low spatial resolution. Thus, improvements in spatial resolution (e.g., by imaging at higher field strengths than clinically used such as 7-T, by use of navigator sequences) are necessary to improve the ability of contrast-enhanced CMR imaging to visualize structural changes after ME in vivo. Whether the detection of LGE might contribute to risk stratification after percutaneous coronary intervention and stent implantation in addition to established biomarkers of necrosis needs to be elucidated in patients.

**Reprint requests and correspondence:** Dr. Frank Breuckmann, West German Heart Center Essen, Department of Cardiology, University Duisburg-Essen, Hufelandstr. 55, Essen D-45122, Germany. *E-mail: Frank.Breuckmann@uk-essen.de.*

## REFERENCES

1. Erbel R, Heusch G. Coronary microembolization. J Am Coll Cardiol 2000;36:22–4.
2. Skyschally A, Leineweber K, Gres P, Haude M, Erbel R, Heusch G. Coronary microembolization. Basic Res Cardiol 2006;101:373–82.
3. Hori M, Inoue M, Kitakaze M, et al. Role of adenosine in hyperemic response of coronary blood flow in microembolization. Am J Physiol 1986; 250:H509–18.
4. Dorge H, Neumann T, Behrends M, et al. Perfusion-contraction mismatch with coronary microvascular obstruction: role of inflammation. Am J Physiol Heart Circ Physiol 2000;279: H2587–92.
5. Skyschally A, Schulz R, Erbel R, Heusch G. Reduced coronary and inotropic reserves with coronary microembolization. Am J Physiol Heart Circ Physiol 2002;282:H611–4.
6. Skyschally A, Haude M, Dorge H, et al. Glucocorticoid treatment prevents progressive myocardial dysfunction resulting from experimental coronary microembolization. Circulation 2004; 109:2337–42.
7. Skyschally A, Gres P, Hoffmann S, et al. Bidirectional role of tumor necrosis factor-alpha in coronary microembolization: progressive contractile dysfunction versus delayed protection against infarction. Circ Res 2007;100: 140–6.
8. El-Maraghi N, Genton E. The relevance of platelet and fibrin thromboembolism of the coronary microcirculation, with special reference to sudden cardiac death. Circulation 1980;62:936–44.
9. Falk E. Plaque rupture with severe pre-existing stenosis precipitating coronary thrombosis. Characteristics of coronary atherosclerotic plaques underlying fatal occlusive thrombi. Br Heart J 1983;50:127–34.
10. Falk E. Unstable angina with fatal outcome: dynamic coronary thrombosis leading to infarction and/or sudden death. Autopsy evidence of recurrent mural thrombosis with peripheral embolization culminating in total vascular occlusion. Circulation 1985;71: 699–708.
11. Leach IH, Blundell JW, Rowley JM, Turner DR. Acute ischaemic lesions in death due to ischaemic heart disease. An autopsy study of 333 cases of out-of-hospital death. Eur Heart J 1995;16:1181–5.
12. Johansen O, Brekke M, Stromme JH, et al. Myocardial damage during percutaneous transluminal coronary angioplasty as evidenced by troponin T measurements. Eur Heart J 1998;19: 112–7.
13. Reffelmann T, Kloner RA. The no-reflow phenomenon: a basic mechanism of myocardial ischemia and reperfusion. Basic Res Cardiol 2006; 101:359–72.
14. Bahrmann P, Werner GS, Heusch G, et al. Detection of coronary microembolization by Doppler ultrasound in patients with stable angina pectoris undergoing elective percutaneous coronary interventions. Circulation 2007; 115:600–8.
15. Cavallini C, Rugolotto M, Savonitto S. Prognostic significance of creatine kinase release after percutaneous coronary intervention. Ital Heart J 2005; 6:522–9.
16. Mizote I, Ueda Y, Ohtani T, et al. Distal protection improved reperfusion and reduced left ventricular dysfunction in patients with acute myocardial infarction who had angioscopically defined ruptured plaque. Circulation 2005;112:1001–7.
17. Stone GW, Webb J, Cox DA, et al. Distal microcirculatory protection during percutaneous coronary intervention in acute ST-segment elevation myocardial infarction: a randomized controlled trial. JAMA 2005;293:1063–72.
18. Leineweber K, Bose D, Vogelsang M, Haude M, Erbel R, Heusch G. Intense vasoconstriction in response to aspirate from stented saphenous vein aortocoronary bypass grafts. J Am Coll Cardiol 2006;47:981–6.
19. Bose D, Leineweber K, Konorza T, et al. Release of TNF-alpha during stent implantation into saphenous vein aortocoronary bypass grafts and its relation to plaque extrusion and restenosis. Am J Physiol Heart Circ Physiol 2007;292:H2295–9.
20. Abdel-Aty H, Zagrosek A, Schulz-Menger J, et al. Delayed enhancement and T2-weighted cardiovascular magnetic resonance imaging differentiate acute from chronic myocardial infarction. Circulation 2004;109:2411–6.
21. Ricciardi MJ, Wu E, Davidson CJ, et al. Visualization of discrete microinfarction after percutaneous coronary intervention associated with mild creatine kinase-MB elevation. Circulation 2001;103:2780–3.
22. Choi JW, Gibson CM, Murphy SA, Davidson CJ, Kim RJ, Ricciardi MJ. Myonecrosis following stent placement: association between impaired TIMI myocardial perfusion grade and MRI visualization of microinfarction. Catheter Cardiovasc Interv 2004;61:472–6.

23. Selvanayagam JB, Porto I, Channon K, et al. Troponin elevation after percutaneous coronary intervention directly represents the extent of irreversible myocardial injury: insights from cardiovascular magnetic resonance imaging. Circulation 2005;111: 1027–32.
24. Porto I, Selvanayagam JB, Van Gaal WJ, et al. Plaque volume and occurrence and location of periprocedural myocardial necrosis after percutaneous coronary intervention: insights from delayed-enhancement magnetic resonance imaging, thrombolysis in myocardial infarction myocardial perfusion grade analysis, and intravascular ultrasound. Circulation 2006;114:662–9.
25. Selvanayagam JB, Cheng AS, Jerosch-Herold M, et al. Effect of distal embolization on myocardial perfusion reserve after percutaneous coronary intervention: a quantitative magnetic resonance perfusion study. Circulation 2007;116:1458–64.
26. Kaiser GM, Heuer MM, Fruhauf NR, Kuhne CA, Broelsch CE. General handling and anesthesia for experimental surgery in pigs. J Surg Res 2006;130:73–9.
27. Neumann T, Konietzka I, van de Sand A, Aker S, Schulz R, Heusch G. Identification of necrotic tissue by phase-contrast microscopy at an early stage of acute myocardial infarction. Lab Invest 2000;80:981–2.
28. Cerqueira MD, Weissman NJ, Dilsizian V, et al. Standardized myocardial segmentation and nomenclature for tomographic imaging of the heart: a statement for healthcare professionals from the Cardiac Imaging Committee of the Council on Clinical Cardiology of the American Heart Association. Circulation 2002;105:539–42.
29. Wagner A, Mahrholdt H, Holly TA, et al. Contrast-enhanced MRI and routine single photon emission computed tomography (SPECT) perfusion imaging for detection of subendocardial myocardial infarcts: an imaging study. Lancet 2003;361: 374–9.
30. Kellman P, Aletras AH, Mancini C, McVeigh ER, Arai AE. T2-prepared SSFP improves diagnostic confidence in edema imaging in acute myocardial infarction compared to turbo spin echo. Magn Reson Med 2007;57: 891–7.

**Key Words:** coronary microembolization ■ magnetic resonance imaging ■ contractile dysfunction ■ late gadolinium enhancement.